View metadata, citation and similar papers at core.ac.uk

brought to you by CORE

provided by St Andrews Research Repository

Irreversible magnetization switching at the onset of superconductivity in a superconductor ferromagnet hybrid

P. J. Curran, J. Kim, N. Satchell, J. D. S. Witt, G. Burnell, M. G. Flokstra, S. L. Lee, J. F. K. Cooper, C. J. Kinane , S. Langridge, A. Isidori, N. Pugach, M. Eschrig, and S. J. Bending

Citation: Applied Physics Letters **107**, 262602 (2015); doi: 10.1063/1.4938467
View online: http://dx.doi.org/10.1063/1.4938467
View Table of Contents: http://scitation.aip.org/content/aip/journal/apl/107/26?ver=pdfcov
Published by the AIP Publishing

Articles you may be interested in

Reentrant superconductivity and superconducting critical temperature oscillations in F/S/F trilayers of Cu41Ni59/Nb/Cu41Ni59 grown on cobalt oxide
J. Appl. Phys. **114**, 033903 (2013); 10.1063/1.4813131

The Volleben effect in magnetic superconductors Dy1− x Y x Rh4B4 (x=0.2, 0.3, 0.4, and 0.6)
Low Temp. Phys. **38**, 154 (2012); 10.1063/1.3681903

Superconductivity in the vicinity of ferromagnetism in oxygen free perovskite MgCNi3: An experimental and density functional theory study
J. Appl. Phys. **111**, 033907 (2012); 10.1063/1.3679564

Giant conductance anisotropy in magnetically coupled Ferromagnet-Superconductor-Ferromagnet structures
Appl. Phys. Lett. **96**, 092513 (2010); 10.1063/1.3352079

Structural, Transport and Magnetic Properties of the Doped Magnetic Superconductor Ru-1212
AIP Conf. Proc. **678**, 333 (2003); 10.1063/1.1612401

This article is copyrighted as indicated in the article. Reuse of AIP content is subject to the terms at: http://scitation.aip.org/termsconditions. Downloaded to IP: 138.251.162.186 On: Fri, 29 Jan 2016 15:21:14

Irreversible magnetization switching at the onset of superconductivity in a superconductor ferromagnet hybrid

P. J. Curran,[1] J. Kim,[2] N. Satchell,[2] J. D. S. Witt,[2] G. Burnell,[2] M. G. Flokstra,[3] S. L. Lee,[3] J. F. K. Cooper,[4] C. J. Kinane,[4] S. Langridge,[4] A. Isidori,[5] N. Pugach,[5,6] M. Eschrig,[5] and S. J. Bending[1]

[1]*Department of Physics, University of Bath, Claverton Down, Bath BA2 7AY, United Kingdom*
[2]*School of Physics and Astronomy, University of Leeds, Leeds LS2 9JT, United Kingdom*
[3]*School of Physics and Astronomy, SUPA, University of St. Andrews, St. Andrews KY16 9SS, United Kingdom*
[4]*ISIS, Rutherford Appleton Laboratory, Oxfordshire OX11 0QX, United Kingdom*
[5]*Department of Physics, Royal Holloway, University of London, Egham, Surrey TW20 0EX, United Kingdom*
[6]*Skobeltsyn Institute of Nuclear Physics, M.V. Lomonosov Moscow State University (SYNP MSU), Leninskie Gory, Moscow 119991, Russia*

(Received 29 October 2015; accepted 9 December 2015; published online 31 December 2015)

We demonstrate that the magnetic state of a superconducting spin valve, that is normally controlled with an external magnetic field, can also be manipulated by varying the temperature which increases the functionality and flexibility of such structures as switching elements. In this case, switching is driven by changes in the magnetostatic energy due to spontaneous Meissner screening currents forming in the superconductor below the critical temperature. Our scanning Hall probe measurements also reveal vortex-mediated pinning of the ferromagnetic domain structure due to the pinning of quantized stray fields in the adjacent superconductor. The ability to use temperature as well as magnetic field to control the local magnetisation structure raises the prospect of potential applications in magnetic memory devices. © *2015 AIP Publishing LLC*.
[http://dx.doi.org/10.1063/1.4938467]

Recent decades have witnessed the invention of many ferromagnetic and superconducting devices for key applications in sensing[1] and data storage.[2] Early developments were based on a single functional material as it was generally assumed that superconductivity (S) and ferromagnetism (F) were antagonistic phenomena whose order parameters were incompatible.[3] In the last 10 years, however, it has become increasingly clear that hybrid S/F structures can play host to a plethora of exotic phenomena whose unique properties afford possibilities for novel applications and devices.[4,5]

To date, nearly all of the applications of S-F hybrids exploit the *influence of a ferromagnet on a superconductor*, but in the last few years' attention has also begun to turn to the reverse situation, the *influence of a superconductor on a ferromagnet*. The observed phenomena can be loosely classified into two groups: Abrikosov vortex mediated pinning of ferromagnetic domains[6] and the restructuring of ferromagnetic domains due to changes in magnetostatic energy arising from Meissner shielding currents flowing in a nearby superconductor.[7–10] In this letter, we demonstrate how both of these phenomena can be observed in a single device and we demonstrate how a dramatic *irreversible* change in the magnetization of the F layer can be induced by cycling an adjacent S layer below its critical temperature (T_c). Hence the switch is dependent on external field *and* temperature, increasing its functionality and flexibility as a potential switching element for use in memory arrays and superconducting spintronic devices.[11]

Scanning Hall probe microscopy (SHPM) has been used to image the *perpendicular* stray magnetic fields emanating from the surface of a superconducting spin valve. SHPM is a non-invasive technique that measures the *spatially resolved* magnetic induction presented as a 2D image where the greyscale, ΔB, signifies the relative difference between the maximum and minimum induction in the image. A Hall effect sensor with an active width $w \approx 500\,\text{nm}$ has been fabricated in the two-dimensional electron gas of an AlGaAs/GaAs heterostructure using a combination of optical and electron beam lithography, wet chemical etching, and metal deposition.

The spin valve stack studied here (Fig. 1 inset) was originally conceived for a series of experiments in superconducting spintronics,[5] and it should be noted that the phenomena described here could equally well be observed in a simple S/F bilayer. Samples were prepared by dc magnetron sputtering in a system with a base pressure of 10^{-8} mbar and a typical growth rate of $\sim 2\,\text{Å}\,\text{s}^{-1}$. The principal elements of the device are the superconductor (S), the "free" ferromagnet (F1), and the "pinned" ferromagnet (F2) layers. The lower half of the stack uses the exchange bias of the antiferromagnet to pin the magnetization of F2, while the direction of the moment F1 can readily be manipulated via small external in-plane magnetic fields. Deposition is performed in the presence of a constant in-plane magnetic field which defines the easy direction of the pinned moment. A very thin non-superconducting Nb spacer layer magnetically decouples the free and pinned moments. The 500 Å superconducting Nb layer has a critical temperature of $T_c = 7.8\,\text{K}$.

Fig. 1(a) shows a magnetization loop for an in-plane field, obtained with vibrating sample magnetometry (VSM) at 10 K. The magnetization jumps correspond to reversal of the Co moments, and the height of the jumps can be linked to the thicknesses of specific Co layers. This allows one to

 © 2015 AIP Publishing LLC

This article is copyrighted as indicated in the article. Reuse of AIP content is subject to the terms at: http://scitation.aip.org/termsconditions. Downloaded to IP: 138.251.162.186 On: Fri, 29 Jan 2016 15:21:14

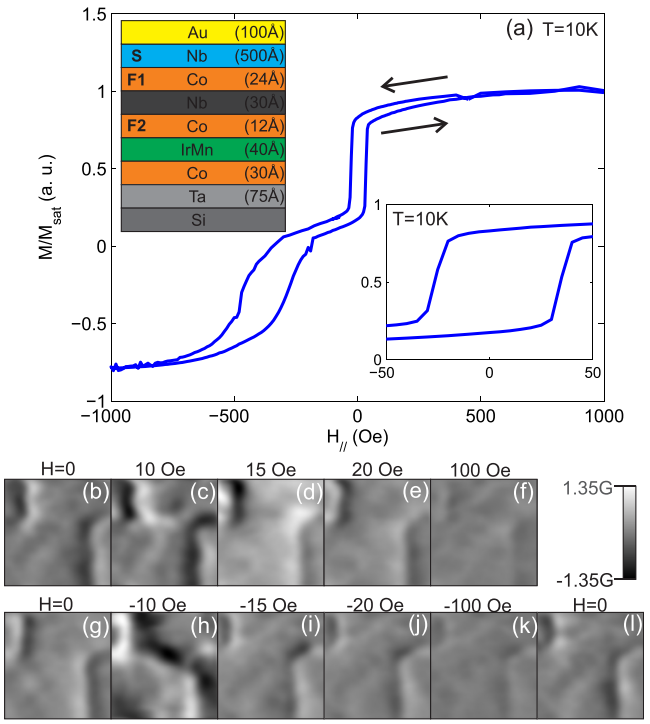

FIG. 1. (a) T = 10 K VSM characterisation of the spin-valve displaying the sharp switching of the "free" moment F1 at low fields. The inset shows an enlarged view of the F1 layer switching. (b)–(l) A sequence of SHPM images (20 μm × 20 μm) at different applied fields through reversal of the free moment at T = 77 K. (b) is taken after negative saturation.

infer that the sharp switching of the free layer occurs at $H_c^{F1}(10\,K) \approx \pm 25$ Oe (inset), and the slower gradual switching of the exchange biased buffer layer between ~ -300 Oe and -500 Oe. The thinner pinned moment, F2, is unaffected at these measurement fields confirming the correct operation of the device.

Panels (b) to (l) show SHPM images, taken at 77 K to take advantage of the larger scan size at this temperature, at various points on a minor loop around the free layer switching field ($H_c^{F1}(77\,K) \approx \pm 14$ Oe). The free layer is almost saturated at ± 100 Oe, and hence very little magnetic structure is observed at these fields, (f) and (k). The structure that does remain is attributed to magnetic roughness due to the polycrystalline nature of the IrMn exchange bias layer. However, at zero field, several strong remnant magnetic features are visible in the image which evolve as the applied field is increased.

Other examples of remnant magnetic objects are displayed in Fig. 2, and we interpret them as 360° domain walls (360DW), which are frequently observed in ferromagnetic

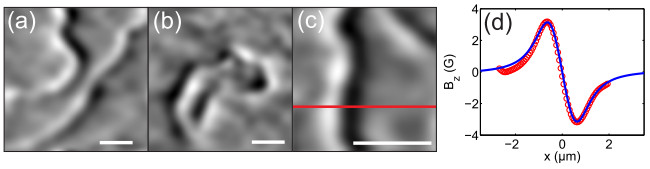

FIG. 2. Typical SHPM images of 360DWs in the 2.4 nm free Co layer of our sample at remanence after saturation in positive fields at 77 K, (a) and (b), and at 10 K (c) (scale bars 5 μm). (d) Shows a theoretical fit to the line scan indicated in (c).

thin films with in-plane anisotropy[12] and often form during reversal around defects which pin local moments.[13] Fig. 2(d) shows a fit to the experimental signal above a 360DW whose magnetization $\mathbf{M}(\mathbf{r})$ is described by

$$\boldsymbol{M}(\boldsymbol{r}) = M_0 \begin{pmatrix} -\mathrm{sech}\left(\dfrac{x+\frac{S}{2}}{\Delta}\right) + \mathrm{sech}\left(\dfrac{x-\frac{S}{2}}{\Delta}\right) \\ \tanh\left(\dfrac{x+\frac{S}{2}}{\Delta}\right) + \tanh\left(\dfrac{x-\frac{S}{2}}{\Delta}\right) \\ 0 \end{pmatrix}, \quad (1)$$

where M_0 is the magnitude of the magnetization, Δ is the domain wall width, and S is the lateral spacing of the two 180° walls. The magnetic induction above the 360DW is evaluated from (1) and the standard relation for the field due to a magnetic dipole moment.[14]

The excellent fit shown in Fig. 2(d) confirms the presence of 360DWs and has been achieved with the physically reasonable fitting parameters, $\Delta = 5$ nm and $S = 700$ nm. Here, $M_0 = 1.1 \times 10^6\,A\,m^{-1}$ is the saturation magnetization of our d = 24 Å Co film,[15] and the fit includes corrections for the sensor scan height ($z_0 = 900$ nm) and active Hall probe width ($w = 500$ nm).

Fig. 3 shows a sequence of images as the magnitude of the in-plane field is increased through the switching field of the free layer ($H_c^{F1}(10\,K) \approx \pm 25$ Oe). The applied field is collinear with the pinned moment, which is horizontal in the image frame. After saturation (a), the initial remnant state (b) shows a 360DW wrapped around a strong pinning site in a spiral pattern. Increases in |H| below the switching field $|H_c^{F1}|$ induce minimal changes in the magnetic structure c.f., images (b) to (d). At H = −25 Oe (e), a dramatic rearrangement of the 360DW from a spiral into an approximately linear wall running diagonally across the image is observed. The switch of the free moment direction from left-to-right to right-to-left across the image is apparent in the reversal of the dipole signature across the 360DW structures from (left-hand-side/right-hand-side) black/white in (d), before the switch, to white/black in (f), after the switch. Therefore, we can establish a clear link between the direction of the F1 moment and the image contrast. The image pattern is

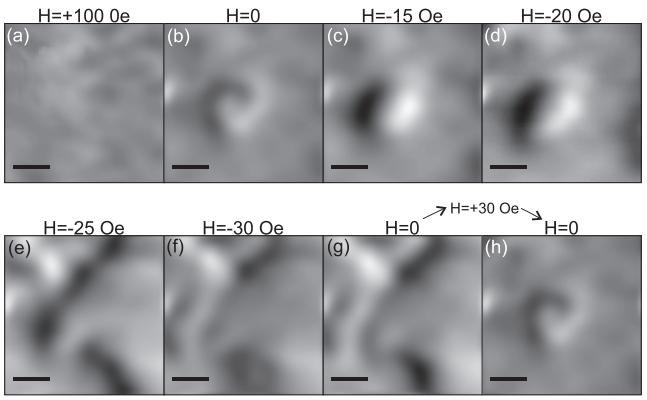

FIG. 3. T = 10 K. A sequence of SHPM images (scale bar 2 μm) at different fields, capturing the evolution of a 360DW during reversal of the free layer moment ($H_c^{F1}(10\,K) \approx \pm 25$ Oe). Image greyscales ΔB span ≈ 3 G to 8 G.

This article is copyrighted as indicated in the article. Reuse of AIP content is subject to the terms at: http://scitation.aip.org/termsconditions. Downloaded to IP: 138.251.162.186 On: Fri, 29 Jan 2016 15:21:14

approximately unchanged after further increases in the field magnitude up to 100 Oe (images not shown) and on subsequent removal of the field (g).

The two remnant 360DW structures shown in (b) and (g) are remarkably reproducible and can be retrieved indefinitely by applying small switching fields of ±30 Oe, as shown by image (h), taken after H = +30 Oe has been applied and zeroed.

The reproducible behaviour of the 360DWs at temperatures above the T_c of Nb is in marked contrast to that below T_c. Fig. 4 shows a sequence where the temperature is dropped below T_c at each field step. This alters the magnetostatic energy of the system as spontaneous Meissner currents flow in the plane of the film, expelling field lines and exerting a magnetostatic force on the adjacent ferromagnetic domains. The screening is small because the thickness of the S layer is comparable to the London penetration depth. Hence images captured above and below T_c tend to look qualitatively similar, c.f., Figs. 4(b) and 4(c). However, the screening is reflected in a drop in the image greyscale (ΔB) of ∼50%.

At 15 Oe, there is no discernible change to the magnetic structure as T is cycled below T_c, (b) to (d). However, at 20 Oe, still 5 Oe *below* the device switching field, there is a dramatic reorganisation of the magnetic structure in the image when $T < T_c$, (f). Furthermore, upon returning to $T > T_c$, (g), we notice that the previous structure is not recovered and an *irreversible* change to the magnetic structure has occurred. Clearly, the change in magnetostatic energy has triggered a change in the domain structure of the free layer. Note also that the domain pattern remains invariant for a subsequent field increase up to 30 Oe, and that the strong dipole-like feature in the lower left quadrant of (e) is (left-hand-side/right-hand-side) white/black while in (g) the resulting dipole at the right lower edge has reversed to black/white. This indicates that the reorganisation that occurred between (e) and (g) was associated with local reversal of the F1 layer moment.

The influence of the superconductor on the ferromagnet can also be demonstrated via a second independent phenomenon, *Abrikosov-vortex mediated pinning of the ferromagnetic domains*. The sequence shown in Fig. 5 again repeats that of

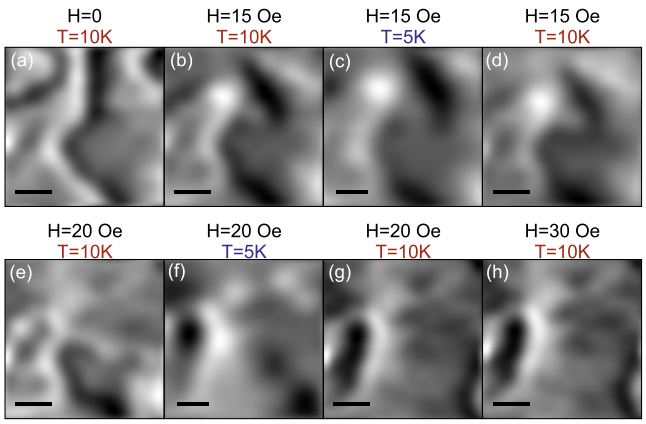

FIG. 4. A sequence of SHPM images (scale bar 2 μm) illustrating magnetostatic domain restructuring. Cycling the temperature from the normal state to $T < T_c$ has no effect at 15 Oe, but triggers a dramatic rearrangement in the ferromagnetic domain structure at 20 Oe, when the field is still ∼5 Oe below the device switching field ($H_c^{F1}(10\,K) \approx \pm 25$ Oe).

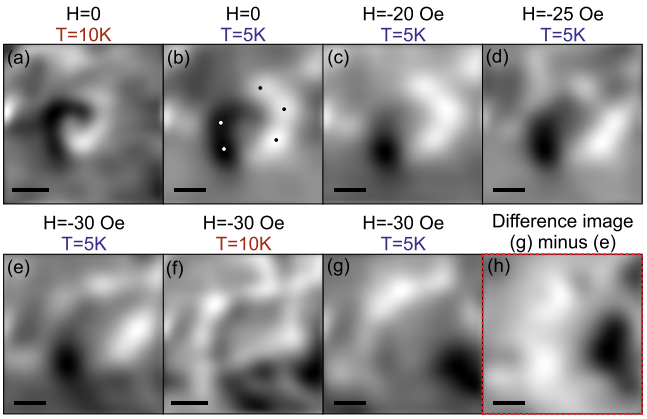

FIG. 5. A sequence of SHPM images (scale bar 2 μm) illustrating vortex mediated domain pinning with fields applied collinear to the pinned moment. Below T_c, the ferromagnetic domain structure remains qualitatively unchanged in applied fields in excess of the device switching field (c). However, cycling to $T > T_c$ triggers a dramatic rearrangement of the stray fields at the surface (d).

Fig. 3, but now T = 5 K and the Nb remains superconducting while the applied field is increased. On cooling below T_c, the stray fields from the spiral domain in the F1 layer, Fig. 5(a), are forced to quantize into superconducting vortices, (b). Here, we observe the coexistence of vortices and antivortices, highlighted by black and white dots, respectively, which has already been predicted,[16] and observed,[17] in SF bi-layers.

In marked contrast to the behavior at T = 10 K, the magnetic structure remains qualitatively unchanged as the field is stepped up to 30 Oe, 5 Oe *in excess* of the known switching field. However, as the temperature is cycled to $T > T_c$ and back to 5 K, a dramatic reorganization of the flux pattern is observed, *at a fixed applied field*, which is best shown by the difference image (red border). Note that there is no appreciable change in the coercive field in these devices over this temperature range and that small changes in the number of vortices in the images (c) to (e) are attributable to an unavoidable out-of-plane component of the nominally in-plane field due to coil/sample misalignment.

Finally, Fig. 6 demonstrates the vortex pinning phenomena via azimuthal rotation of an in-plane field of fixed magnitude. In this sequence, a 90° rotation of a 100 Oe in-plane field from collinear with the pinned moment (horizontal in the image frame) to perpendicular to it (vertical in the image frame) and back again, (a) to (c), produces a reversible change in the domain structure above T_c. However, when the same cycle is performed below T_c, we observe no change in the image contrast for a 90° rotation, (d) to (e), and the original rotated state is only retrieved upon warming to $T > T_c$ (i.e., (b) and (f) are almost identical). Panels (g) and (h) show the average induction (⟨B⟩) and greyscale (ΔB) from a typical sequence of images, for a 180° rotation of the in-plane field. Above T_c, there are appreciable changes in both and ΔB during rotation of H which are attributable to changes in the magnetic structure, c.f., Fig. 6 panels (a) and (b). Below T_c, there are no significant changes in or ΔB confirming that the flux pattern is completely locked in for rotations of a 100 Oe field in the range −90 to +90°.

The change in magnetostatic energy of an S/F bilayer system, due to the Meissner shielding of the S layer, was

This article is copyrighted as indicated in the article. Reuse of AIP content is subject to the terms at: http://scitation.aip.org/termsconditions. Downloaded to IP: 138.251.162.186 On: Fri, 29 Jan 2016 15:21:14

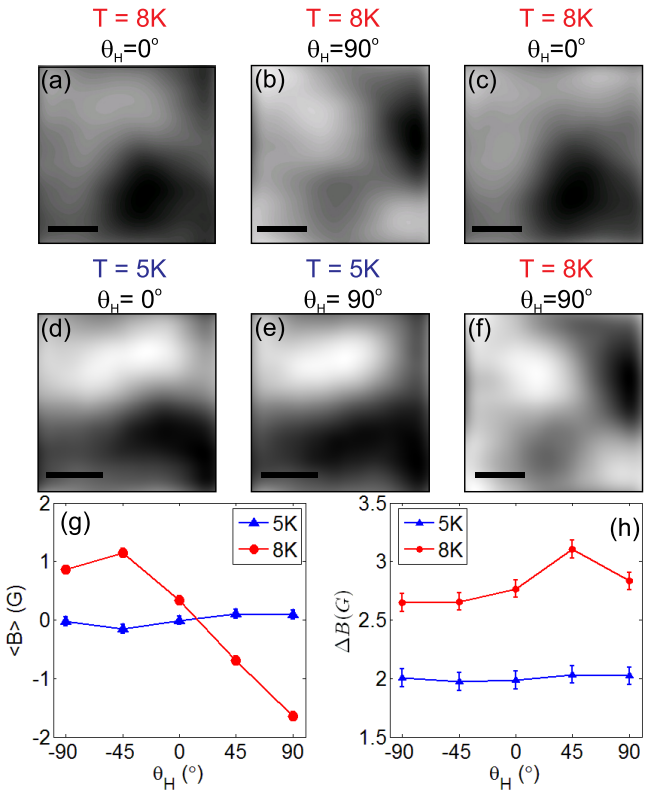

FIG. 6. A sequence of SHPM images (scale bar 2 μm) illustrating the *vortex mediated domain pinning* effect under rotation of the free layer in an applied field of 100 Oe from collinear with the pinned moment ($\theta_H = 0°$), to perpendicular to it ($\theta_H = 90°$). The reversible rearrangements of the domain pattern at 8 K, (a)–(c), are not seen at 5 K, (d) and (e), due to vortex mediated pinning of domains in the free Co layer. The rotated magnetic state is recovered on raising the temperature to 8 K (f). Image greyscales ((a)–(f)) ~0.13 G–0.19 G. (g) The average induction and (h), the image greyscale as a function of angle of applied field.

predicted to cause an appreciable shrinkage of the characteristic domain size in the F layer.[7,18] Indirect experimental evidence of this effect was observed by Dubonos *et al.*,[8] and the shrinkage ratio was later confirmed directly by the careful work of Tamegai *et al.*[10] However, nearly all of the theoretical and experimental investigations to date involve the case where the F layer magnetization is *perpendicular* to the S layer, and the changes in the F domain structure are fully *reversible*. Here, we demonstrate a highly *irreversible* change in an F layer with *parallel* magnetization (Fig. 4). A similar phenomenon *has* been reported in Nb/Co multilayers,[9] but in this instance, the domain reordering took the form of minor incremental shifts in the F layer, over *multiple* successive temperature cycles, and no real-space imaging was performed. In contrast, here we induce the complete 180° reversal of the F moment by lowering the adjacent Nb film into the superconducting state and back out again.

Vortex mediated pinning of ferromagnetic domains (Fig. 5) is a second way that a ferromagnet can be influenced by an adjacent superconductor. The only prior experimental evidence for this effect comes from scanning Hall probe measurements of a Nb/$BaFe_{12}O_{19}$ (S/F) bilayer,[6] where the F moments are perpendicular to the surface and domain pinning alters the relaxation of the domain structure. Here, we are able to observe the quantization of F layer stray fields into superconducting vortices (Fig. 5(a)) on cooling to $T < T_c$. It is the subsequent strong pinning of these vortices at defects in the sputtered Nb film which causes the locking of the observed domain structure at fields in excess of H_c^{F1} (Fig. 5) when a dramatic change in the structure is observed for $T > T_c$ (Fig. 3). Finally, we also demonstrate the robustness of the domain pinning by showing that the domain structure remains unchanged when an applied field of 100 Oe is rotated through 180° at $T < T_c$ (Fig. 6).

In conclusion, we have observed two physical phenomena, magnetostatic domain reordering *and* vortex mediated domain pinning, which arise from the influence of a superconductor on a ferromagnet in a single S/F hybrid device. We have further demonstrated how they can be used to affect the operation of our superconducting spin valve, raising the prospect that they can be utilized to increase the functionality of switching elements in superconducting spintronic and memory array devices. A further natural extension of this work would be to attempt to realize F layer switching via the spin-transfer-torque due to polarized (spin-triplet) supercurrents generated in S/F hybrids with non-collinear moments.[19]

The authors acknowledge financial support from: EPSRC in the UK under Grant Nos. EP/G036101/1, EP/J010626/1, EP/J010634/1, EP/J01060X/1; The NanoSC COST Action MP-1201; A JEOL Europe studentship under Grant No. EP/I000933/1, plus support from the STFC ISIS neutron and muon source. Finally, from RFBR in Russia under 15-52-10045_Ko-a.

[1]P. Grunberg, Acta Mater. **48**(1), 239 (2000); J. R. Kirtley, M. B. Ketchen, K. G. Stawiasz, J. Z. Sun, W. J. Gallagher, S. H. Blanton, and S. J. Wind, Appl. Phys. Lett. **66**(9), 1138 (1995); J. S. Moodera, L. R. Kinder, T. M. Wong, and R. Meservey, Phys. Rev. Lett. **74**(16), 3273 (1995); Y. W. Wang, P. J. Zhou, L. F. Wei, B. H. Zhang, Q. Wei, J. Q. Zhai, W. W. Xu, and C. H. Cao, Phys. C **515**, 49 (2015).
[2]T. D. Clark and J. P. Baldwin, Electron. Lett. 3(5), 178 (1967); J. M. Daughton, Thin Solid Films 216(1), 162 (1992); D. Drung, in *Squid Sensors: Fundamentals, Fabrication and Applications*, edited by H. Weinstock (Kluwer Academic Publications, Dordrecht, 1996), Vol. 329, pp. 63; S. S. P. Parkin, M. Hayashi, and L. Thomas, Science 320(5873), 190 (2008).
[3]V. L. Ginzburg, Sov. Phys. - JETP. **4**(3), 153 (1957).
[4]F. S. Bergeret, A. F. Volkov, and K. B. Efetov, Rev. Mod. Phys. **77**(4), 1321 (2005); M. Eschrig, Rep. Prog. Phys. **78**(10), 104501 (2015); J. I. Martin, M. Velez, J. Nogues, and I. K. Schuller, Phys. Rev. Lett. **79**(10), 1929 (1997); J. W. A. Robinson, S. Piano, G. Burnell, C. Bell, and M. G. Blamire, Phys. Rev. Lett. **97**(17), 177003 (2006); Z. R. Yang, M. Lange, A. Volodin, R. Szymczak, and V. V. Moshchalkov, Nat. Mater. **3**(11), 793 (2004).
[5]M. G. Flokstra, T. C. Cunningham, J. Kim, N. Satchell, G. Burnell, P. J. Curran, S. J. Bending, C. J. Kinane, J. F. K. Cooper, S. Langridge, A. Isidori, N. Pugach, M. Eschrig, and S. L. Lee, Phys. Rev. B. **91**(6), 060501 (2015); M. G. Flokstra, N. Satchell, J. Kim, G. Burnell, P. J. Curran, S. J. Bending, J. F. K. Cooper, C. J. Kinane, S. Langridge, A. Isidori, N. Pugach, M. Eschrig, H. Luetkens, A. Suter, T. Prokscha, and S. L. Lee, "Remotely induced magnetism in a normal metal using a superconducting spin-valve," Nat. Phys. (published online 2015).
[6]J. Fritzsche, R. B. G. Kramer, and V. V. Moshchalkov, Phys. Rev. B **79**(13), 132501 (2009).
[7]L. N. Bulaevskii and E. M. Chudnovsky, Phys. Rev. B **63**(1), 012502 (2001).
[8]S. V. Dubonos, A. K. Geim, K. S. Novoselov, and I. V. Grigorieva, Phys. Rev. B **65**(22), 220513 (2002).
[9]C. Monton, F. de la Cruz, and J. Guimpel, Phys. Rev. B **77**(10), 104521 (2008).
[10]T. Tamegai, Y. Nakao, S. Mohan, and Y. Nakajima, Supercond. Sci. Technol. **24**(2), 024015 (2011).

This article is copyrighted as indicated in the article. Reuse of AIP content is subject to the terms at: http://scitation.aip.org/termsconditions. Downloaded to IP: 138.251.162.186 On: Fri, 29 Jan 2016 15:21:14

[11]J. Y. Gu, C. Y. You, J. S. Jiang, J. Pearson, Y. B. Bazaliy, and S. D. Bader, Phys. Rev. Lett. **89**(26), 267001 (2002); S. Oh, D. Youm, and M. R. Beasley, Appl. Phys. Lett. **71**(16), 2376 (1997); L. R. Tagirov, Phys. Rev. Lett. **83**(10), 2058 (1999).
[12]H. S. Cho, C. H. Hou, M. Sun, and H. Fujiwara, J. Appl. Phys. **85**(8), 5160 (1999).
[13]T. Schrefl, J. Fidler, and M. Zehetmayer, J. Appl. Phys. **87**(9), 5517 (2000).
[14]D. J. Craik, *Magnetism: Principles and Applications* (Wiley, Chichester, 1995).
[15]A. Hrabec, private communication (2014).
[16]Z. Jing, H. D. Yong, and Y. H. Zhou, Supercond. Sci. Technol. **27**(10), 105005 (2014).
[17]M. Iavarone, A. Scarfato, F. Bobba, M. Longobardi, G. Karapetrov, V. Novosad, V. Yefremenko, F. Giubileo, and A. M. Cucolo, Phys. Rev. B **84**(2), 024506 (2011).
[18]G. M. Genkin, V. V. Skuzovatkin, and I. D. Tokman, J. Magn. Magn. Mater. **130**(1–3), 51 (1994); E. B. Sonin, Phys. Rev. B **66**(13), 136501 (2002).
[19]X. Waintal and P. W. Brouwer, Phys. Rev. B **65**(5), 054407 (2002); E. Zhao and J. A. Sauls, Phys. Rev. B **78**(17), 174511 (2008).

This article is copyrighted as indicated in the article. Reuse of AIP content is subject to the terms at: http://scitation.aip.org/termsconditions. Downloaded to IP: 138.251.162.186 On: Fri, 29 Jan 2016 15:21:14